A Multiscale Sub-Octave Wavelet Transform for De-Noising and Enhancement

Andrew F. Laine and Xuli Zong

Department of Computer & Information Science & Engineering
University of Florida, Gainesville, FL 32611
E-mail: laine@cise.ufl.edu, zxl@cise.ufl.edu

ABSTRACT

This paper describes an approach for accomplishing sub-octave wavelet analysis and its discrete implementation for noise reduction and feature enhancement. Sub-octave wavelet transforms allow us to more closely characterize features within distinct frequency bands. By dividing each octave into sub-octave components, we demonstrate a superior ability to capture transient activities in a signal or image more reliably. De-Noising and enhancement are accomplished through techniques of minimizing noise energy and nonlinear processing of transform coefficient energy by gain.

Keywords: Sub-Octave wavelet transform, nonlinear processing, de-noising, contrast enhancement

1 INTRODUCTION

Orthonormal wavelet transforms (OWT) and discrete dyadic wavelet transforms (DWT) have been successful in the analysis of many non-stationary signals.[1–6] In an earlier study, both OWT and DWT were investigated and compared for de-noising and contrast enhancement performance.[7] A DWT designed with a wavelet as the first order derivative of a smoothing function can characterize feature energy from noise energy.[7,8] The separation is used to identify wavelet coefficients to modify in order to enhance specific features of interest (FOI) without amplifying noise. The mother wavelet selected was a smooth and antisymmetric function with few oscillations, which kept de-noising under a DWT less affected from pseudo-Gibbs phenomenon. Such artifacts were evident under an OWT[9,10] compared to similar de-noising results obtained under a DWT.[7] The discrete filters used to compute the DWT had compact support requiring few taps. DWT wavelet coefficients have a clear meaning for analysis in that they are proportional to the image intensity changes (gradients). We show that salient features, such as edges or object boundaries, can be distinguished in a multiscale time-frequency representation of wavelets. By properly modifying signal and noise energy, we can achieve distinct noise reduction and feature enhancement for specific imaging modalities.

A framework for multiscale wavelet analysis was previously implemented for contrast enhancement with noise suppression.[11,12] In this paper, we address both signal or image restoration and enhancement problems via methods of wavelet shrinkage and feature emphasis. Our approach takes advantage of both soft thresholding and hard thresholding wavelet shrinkage techniques to eliminate noise while preserving the sharpness of prominent features. It also incorporates local energy gain for nonlinear processing to enhance contrast within structures and along object boundaries.[7,8]

0-8194-2213-4/96/$6.00

We suggest that a DWT has a limited ability to characterize features, such as texture, and subtle features of importance in mammographic images. The traditional DWT is an octave-based transform where scales increase as powers of two.[5] We suggest that the best representation of a signal's details may exist between two consecutive levels of scale within a DWT. To more reliably isolate noise and identify features through scale space, we use a sub-octave wavelet transform (SWT), which is a generalization of the DWT. A sub-octave wavelet transform provides a means to represent details within sub-octave frequency bands of equally-spaced divisions within each octave band. The theoretical development of a sub-octave wavelet transform and its efficient implementation is described below.

2 SUB-OCTAVE WAVELET TRANSFORM

2.1 Continuous sub-octave wavelet transform

2.1.1 One-Dimensional sub-octave wavelet transform

In this section, we show that when we further divide each octave band into M equally-spaced sub-octave bands, M basis wavelets can be used to capture the detail information of a signal in each sub-octave frequency band. The M wavelet functions are represented as $\psi^m(x) \in L^2(\boldsymbol{R})$, where $m = \{1, 2, .., M\}$. An M-sub-octave wavelet transform of a 1-D function $f(x) \in L^2(\boldsymbol{R})$ at scale 2^j (level j) and location x, for the m-th sub-octave frequency band is defined as

$$W_j^m f(x) \doteq f * \psi_{2^j}^m(x), \tag{1}$$

where $\psi_{2^j}^m(x) = \frac{1}{2^j}\psi^m(\frac{x}{2^j})$ is the dilation of the m-th basis wavelet $\psi^m(x)$, at scale 2^j, $m = \{1, 2, ..., M\}$, and $j \in Z$. The set of frequency responses of $\{\psi_{2^j}^m(x) \mid m = 1, 2, ..., M\}$ for all scales 2^j are required to capture the complete details within any octave. For perfect reconstruction of $f(x)$, analysis wavelets $\psi_{2^j}^m(x)$ and synthesis wavelets $\gamma_{2^j}^m(x)$ should satisfy

$$\sum_{j=-\infty}^{+\infty} \sum_{m=1}^{M} \hat{\psi}^m(2^j\omega)\,\hat{\gamma}^m(2^j\omega) = 1. \tag{2}$$

The reconstruction wavelets $\gamma^m(x)$ can be any function whose Fourier transform satisfies the above equation. There are, in fact, many choices for the decomposition and reconstruction wavelets that satisfy Equation 2. A 1-D sub-octave wavelet transform can be easily extended to a 2-D sub-octave transform by computing sub-octave wavelet coefficients along horizontal and vertical directions, as explained in the following section. Extensions to higher dimensions are analogous.

2.1.2 Two-Dimensional sub-octave wavelet transform

An M-sub-octave wavelet transform of a 2-D function $f(x, y) \in L^2(\boldsymbol{R}^2)$ at scale 2^j (level j) and location (x, y), for the m-th sub-octave frequency band is defined as

$$W_j^{i,m} f(x, y) = f * \psi_{2^j}^{i,m}(x, y), \tag{3}$$

where $\psi_{2^j}^{i,m}(x, y) = \frac{1}{2^{2j}}\psi^{i,m}(\frac{x}{2^j}, \frac{y}{2^j})$, $i = \{1, 2\}$ (for horizontal and vertical directions), $m = \{1, 2, ..., M\}$, and $j \in Z$. For perfect reconstruction of $f(x, y)$, $\psi_{2^j}^m(x, y)$ and synthesis wavelets $\gamma_{2^j}^m(x, y)$ should satisfy

$$\sum_{j=-\infty}^{+\infty} \sum_{i=1}^{2} \sum_{m=1}^{M} \hat{\psi}^{i,m}(2^j\omega_x, 2^j\omega_y)\,\hat{\gamma}^{i,m}(2^j\omega_x, 2^j\omega_y) = 1. \tag{4}$$

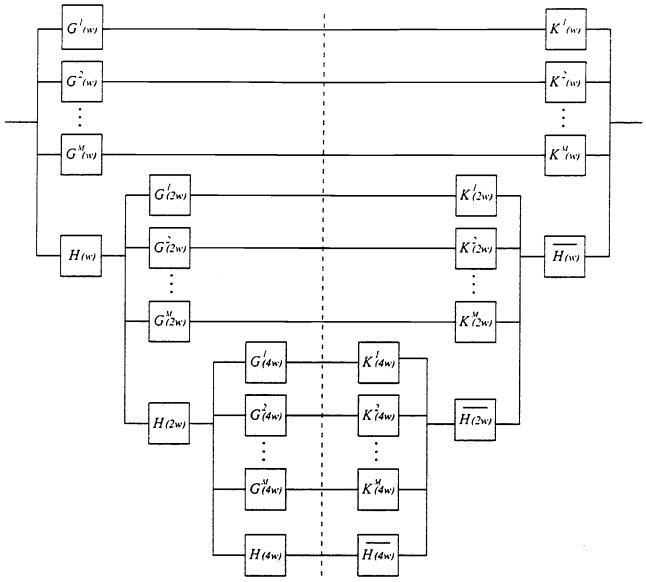

Figure 1: A 3-level SWT decomposition and reconstruction diagram of a 1-D discrete function.

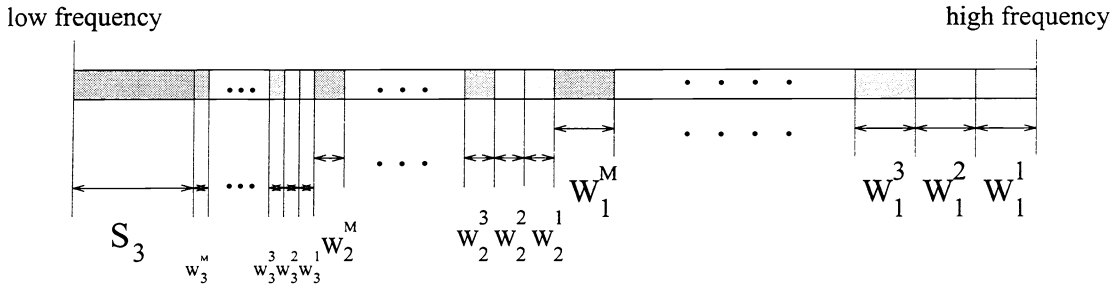

Figure 2: Division of frequency bands under the sub-octave wavelet transform shown in Figure 1.

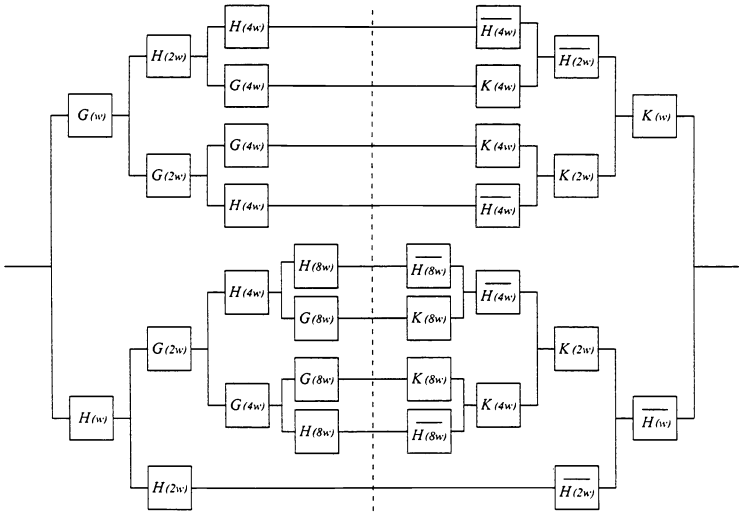

Figure 3: A 2-level 4-sub-octave analysis/synthesis filter bank of a sub-octave wavelet transform.

2.2 Discrete sub-octave wavelet transform

The transform parameters in a sub-octave wavelet transform are continuous variables. This results in a highly redundant representation. It is possible to discretize these parameters and still be able to achieve perfect reconstruction.[13] For digital image processing, the sub-octave wavelet transform of a discrete function can be carried out through uniform sampling of a continuous sub-octave wavelet transform. Below, we describe the discrete formulation of a sub-octave wavelet transform.

2.2.1 One-Dimensional discrete sub-octave wavelet transform

In the discrete domain, we are limited by the finest scale of 1. In general, a discrete function can be decomposed into fine-to-coarse scales. We let $\{ W_j^m f(x_n),\ S_J f(x_n) \mid n \in Z,\ j = 1, 2, ..., J,$ and $m = 1, 2, ..., M \}$ be the wavelet representation of a discrete function $f(x_n)$ under a J-level discrete M-sub-octave wavelet transform. $W_j^m f(x_n)$ and scaling approximation $S_J f(x_n)$ are uniform samplings of their continuous counterparts respectively.

To perform a SWT decomposition and reconstruction, we designed FIR filters (H, G^m, and K^m) which satisfied

$$|H(\omega)|^2 + \sum_{m=1}^{M} G^m(\omega)\, K^m(\omega) = 1. \tag{5}$$

A three-level M-sub-octave wavelet decomposition and reconstruction process is shown in Figure 1. The corresponding division of frequency bands is provided in Figure 2. In general, for M-sub-octave analysis and synthesis of a SWT, we need M pairs of decomposition and reconstruction basis wavelets. A SWT is a multiwavelet transform with a single scaling function.[14,15] When M is a power of 2, we can carry out the decomposition and reconstruction using a set of FIR filters corresponding to a single pair of basis wavelets through frequency band splitting techniques as shown by Daubechies.[2] Figure 3 presents a 2-level 4-sub-octave decomposition and reconstruction of a SWT using FIR filters corresponding to a single pair of basis wavelets.

2.2.2 Two-Dimensional discrete sub-octave wavelet transform

For the decomposition of a 2-D discrete function, we let $\{ W_j^{i,m} f(x_u, y_v), S_J f(x_u, y_v) \mid u, v \in Z, i = 1, 2, j = 1, .., J,$ and $m = 1, .., M \}$ be the wavelet representation of a discrete function $f(x_u, y_v)$ under a 2-D J-level discrete M-sub-octave wavelet transform. In general, $\varphi(x, y)$ is a 2-D scaling function and $\psi^{i,m}(x, y)$ and $\gamma^{i,m}(x, y)$ are the m-th directional analysis and synthesis wavelets. Similar to the way 2-D wavelets are constructed using 1-D wavelets,[5] we used tensor products to construct 2-D sub-octave wavelets using 1-D sub-octave wavelets. Thus we can write

$$\hat{\psi}^{1,m}(2^j\omega_x, 2^j\omega_y) = \hat{\psi}^m(2^j\omega_x)\hat{\varphi}(2^{j-1}\omega_y), \tag{6}$$

$$\hat{\psi}^{2,m}(2^j\omega_x, 2^j\omega_y) = \hat{\varphi}(2^{j-1}\omega_x)\hat{\psi}^m(2^j\omega_y), \tag{7}$$

$$\hat{\varphi}(2^j\omega_x, 2^j\omega_y) = \hat{\varphi}(2^j\omega_x)\hat{\varphi}(2^j\omega_y). \tag{8}$$

Through this construction of 2-D wavelets, we implemented a 2-D sub-octave wavelet transform using 1-D convolution with FIR filters. Figure 4 shows the division of the frequency plane under a 2-level SWT. A 2-D sub-octave wavelet transform was implemented by applying 1-D FIR filters along horizontal and vertical directions.

A dyadic wavelet transform can be a special case of a sub-octave wavelet transform with $M = 1$. As an example, a discrete 2-sub-octave wavelet transform is shown to divide the details of an octave band into details of 2 sub-octave bands. As shown in Figure 5, one sub-octave can be used for detecting local maxima while the other

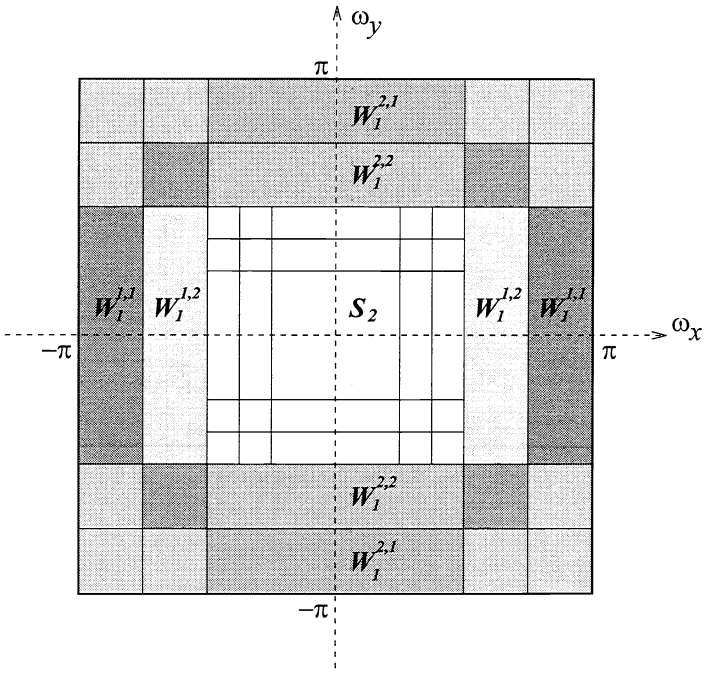

Figure 4: Division of the frequency plane under a 2-D sub-octave wavelet transform.

sub-octave for identifying zero-crossings. The dashed curve is the frequency response of a first order derivative approximation of a smoothing function and the dash-dot curve shows the frequency response of a second order derivative approximation. The solid curve is a scaling approximation of level one. Thus, with these analysis filters we can take advantage of both local maxima and zero-crossing representations to characterize local features emergent within each scale.

3 DE-NOISING AND CONTRAST ENHANCEMENT

3.1 Noise modeling

In general. additive noise can be represented by the following formula:

$$f(\mathbf{x}) = g(\mathbf{x}) + \eta_a(\mathbf{x}), \tag{9}$$

where $g(\mathbf{x})$ is some unknown function. The function $f(\mathbf{x})$ is a noisy observation of $g(\mathbf{x})$, $\eta_a(\mathbf{x})$ is additive noise, and $\mathbf{x}$ is a vector of spatial locations or temporal samples.

For additive noise, there are existing techniques based on mean squared error or methods of l^1 norm optimization to remove noise, such as Donoho's wavelet shrinkage techniques,[9,16,17] Chen and Donoho's basis pursuit de-noising,[18] Mallat's local-maxima-based method for removing white noise,[6] and wavelet packet-based de-noising.[19]

By incorporating a de-noising mechanism into a feature enhancement process, we seek to enhance contrast without amplifying noise. In this section we demonstrate that subtle features barely seen or invisible in a mammogram, such as microcalcification clusters, spicular lesions, and circular (arterial) calcifications, can be enhanced via sub-octave wavelet analysis. Since our algorithm treats noise and features independently, superior

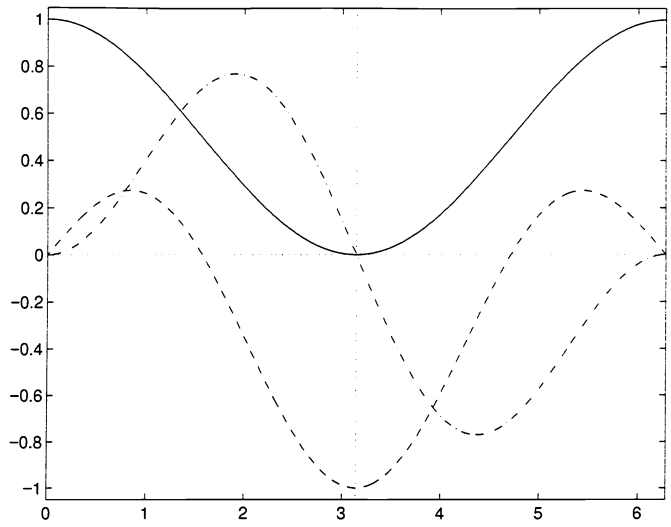

Figure 5: An example of level one analytic filters for 2 sub-octave bands and a low-pass band. The dashed curve is the frequency response of a first order derivative approximation of a smoothing function and the dash-dot curve is the frequency response of a second order derivative approximation. The solid curve is a scaling approximation of level one.

results were obtained compared to existing algorithms designed for enhancement alone.

Below, a de-noising and contrast enhancement scheme based on wavelet shrinkage and feature emphasis is presented. In our investigation, we studied hard thresholding and Donoho's soft thresholding wavelet shrinkage[16] for noise reduction. In our approach for accomplishing de-noising and feature enhancement, we took advantage of both thresholding methods. Donoho's soft thresholding method[16] was developed for an orthonormal wavelet transform[1] primarily with Daubechies's Symmlet 8 basis wavelet. These results showed some undesired side-effects, from pseudo-Gibbs phenomenon.[10] By using a SWT and basis wavelets with fewer oscillations, a result relatively free from side-effects after de-noising was observed. Our experiments showed that a SWT with first and second order derivative approximations of a smoothing function as its basis wavelets separated coefficients characterized by feature energy from coefficients characterized by noise energy. In this algorithm, we adopted regularized soft thresholding wavelet shrinkage to remove noise energy within the finer levels of scale. We then applied to wavelet coefficients within the selected levels of analysis a nonlinear gain with hard thresholding to preserve features while removing small noise perturbations.

3.2 Wavelet shrinkage by soft thresholding

Soft thresholding[16] can be described by

$$u(\mathbf{x}) = \mathcal{T}_S(v(\mathbf{x}), t) = \text{sign}(v(\mathbf{x}))\,(|v(\mathbf{x})| - t)_+, \tag{10}$$

where threshold t is proportional to the noise level and $\mathbf{x} \in D$ where D is the domain of $v(\mathbf{x})$, and $u(\mathbf{x})$ is the result of soft thresholding and has the same sign as $v(\mathbf{x})$ if non-zero. The expression $(|v(\mathbf{x})| - t)_+$ is defined as

$$(|v(\mathbf{x})| - t)_+ = \begin{cases} |v(\mathbf{x})| - t & \text{if } |v(\mathbf{x})| > t, \\ 0 & \text{otherwise.} \end{cases}$$

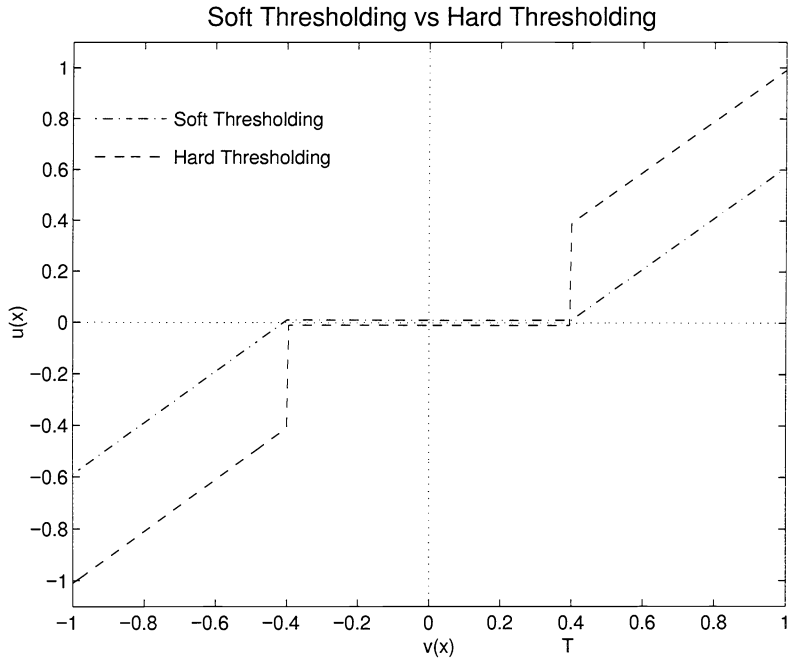

Figure 6: A comparison of thresholding methods.

SWT coefficients were processed for noise reduction by

$$W_j^{i,m,*} f(\mathbf{x}) = \mathcal{T}_S(W_j^{i,m} f(\mathbf{x}), t_{2^j}^{i,m}), \tag{11}$$

where $i = \{1, 2\}$ (omitted for 1-D signals), $j = \{1, ..., k\}$, $k \leq J$, $m = \{1, ..., M\}$, and $t_{2^j}^{i,m}$ is a noise and scale-related threshold. The result $W_j^{i,m,*} f(\mathbf{x})$ is a modified coefficient. Recall that Donoho's soft thresholding method used a single global threshold. However, since noise coefficients under a SWT have average decay through fine-to-coarse scales, we regulated soft thresholding wavelet shrinkage by applying coefficient-dependent thresholds decreasing across scales.

3.3 Coefficient shrinkage by hard thresholding

A hard thresholding operation can be expressed as

$$u(\mathbf{x}) = \mathcal{T}_H(v(\mathbf{x}), t) = v(\mathbf{x})(|v(\mathbf{x})| \geq t), \tag{12}$$

where t is a threshold value, $\mathbf{x} \in D$, the domain of $v(\mathbf{x})$, and $u(\mathbf{x})$ is the result of hard thresholding and has the same sign as $v(\mathbf{x})$ if non-zero. The meaning of $(|v(\mathbf{x})| \geq t)$ is defined by the expression

$$(|v(\mathbf{x})| \geq t) = \begin{cases} 1 & \text{if } |v(\mathbf{x})| \geq t, \\ 0 & \text{otherwise.} \end{cases}$$

Sub-octave wavelet coefficients were modified by hard thresholding for noise reduction by

$$W_j^{i,m,*} f(\mathbf{x}) = \mathcal{T}_H(W_j^{i,m} f(\mathbf{x}), t_{2^j}^{i,m}), \tag{13}$$

where $i = \{1, 2\}$ (omitted for 1-D signals), $j = \{1, ..., k\}$, and $k \leq J$, $m = \{1, ..., M\}$, and $t_{2^j}^{i,m}$ is (in general) a threshold related to noise and scale. Again, the output result $W_j^{i,m,*} f(\mathbf{x})$ is a processed coefficient. Figure 6

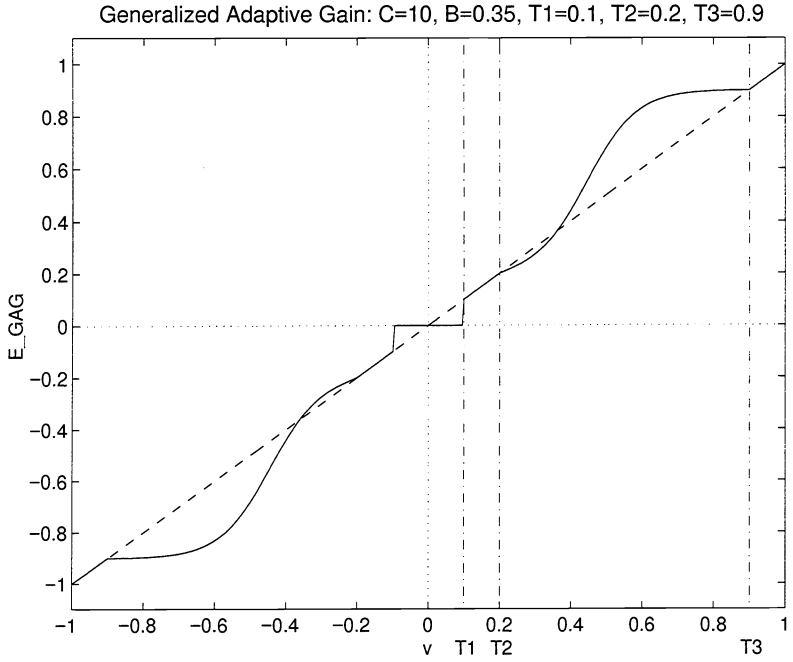

Figure 7: An example of a generalized adaptive gain function.

shows a functional diagram of normalized soft and hard thresholding. When features and noise can be clearly separated at the finer levels of scale, applying hard thresholding instead of soft thresholding may further improve performance.

3.4 Feature emphasis by generalized adaptive gain

Recently, several wavelet-based enhancement techniques have been developed.[20–23] Adaptive gain through nonlinear processing[22,24] has been successfully used to enhance features in digital mammograms. Here, adaptive gain through nonlinear processing is further generalized to incorporate hard thresholding in order to avoid amplifying noise and remove small noise perturbations. The generalized adaptive gain (GAG) nonlinear operator is defined as

$$E_{GAG}(v) = \begin{cases} 0 & \text{if } |v| < T_1, \\ \text{sign}(v)\, T_2 + \bar{a}\,(\text{sigm}(c(u-b)) - \text{sigm}(-c(u+b))) & \text{if } T_2 \le |v| \le T_3, \\ v & \text{otherwise,} \end{cases} \tag{14}$$

where $v \in [-1,\ 1]$, $\bar{a} = a(T_3 - T_2)$, $u = \text{sign}(v)(|v| - T_2)/(T_3 - T_2)$, $b \in (0,\ 1)$, $0 \le T_1 \le T_2 < T_3 \le 1$, c is a gain factor, and a can be computed by

$$a = \frac{1}{\text{sigm}(c(1-b)) - \text{sigm}(-c(1+b))}, \tag{15}$$

$$\text{sigm}(v) = \frac{1}{1+e^{-v}}. \tag{16}$$

Parameters T_1, T_2, and T_3 are selected values. When $T_1 = T_2 = 0$ and $T_3 = 1$, the expression is equivalent to an adaptive gain nonlinear function used previously.[22,24] The interval $[T_2,\ T_3]$ serves as a sliding window for feature selectivity. It can be adjusted to emphasize coefficients within a specific range of variation. Thus, by selecting

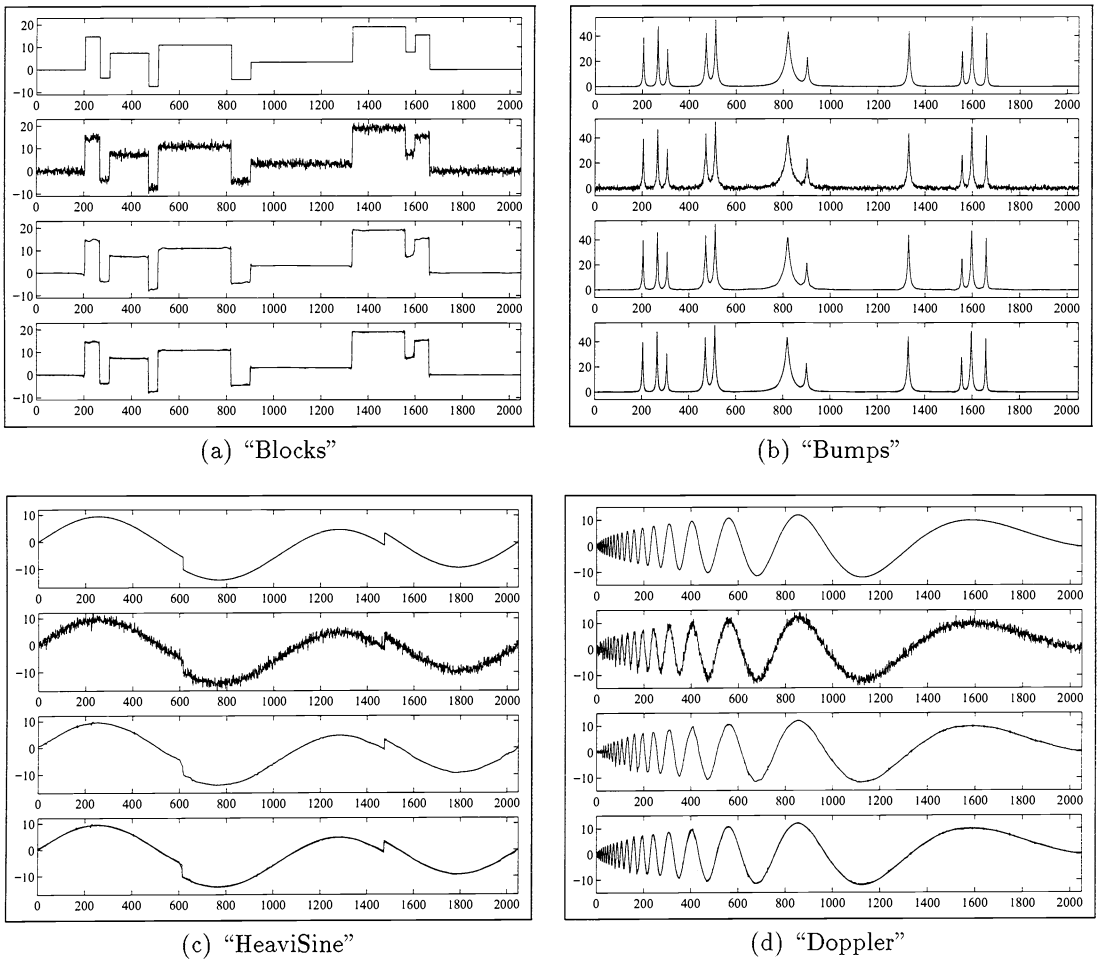

(a) "Blocks" (b) "Bumps"

(c) "HeaviSine" (d) "Doppler"

Figure 8: De-Noised and restored features from the SWT-based algorithm from top to bottom: original signal; noisy signal; de-noised signal; overlay of original and de-noised signal.

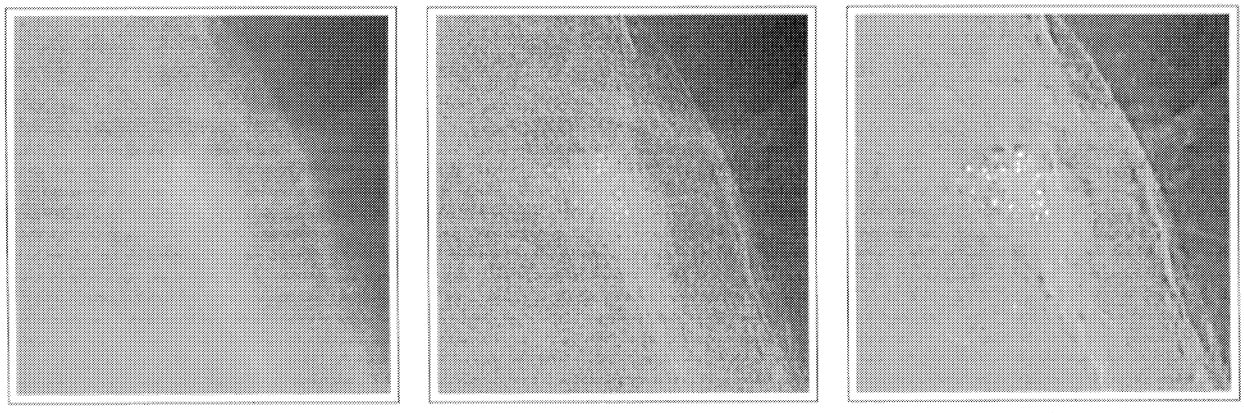

(a) (b) (c)

Figure 9: (a) Area of a low contrast mammogram with a microcalcification cluster. (b) Best enhancement by traditional unsharp masking. (c) SWT-based enhancement with noise suppression.

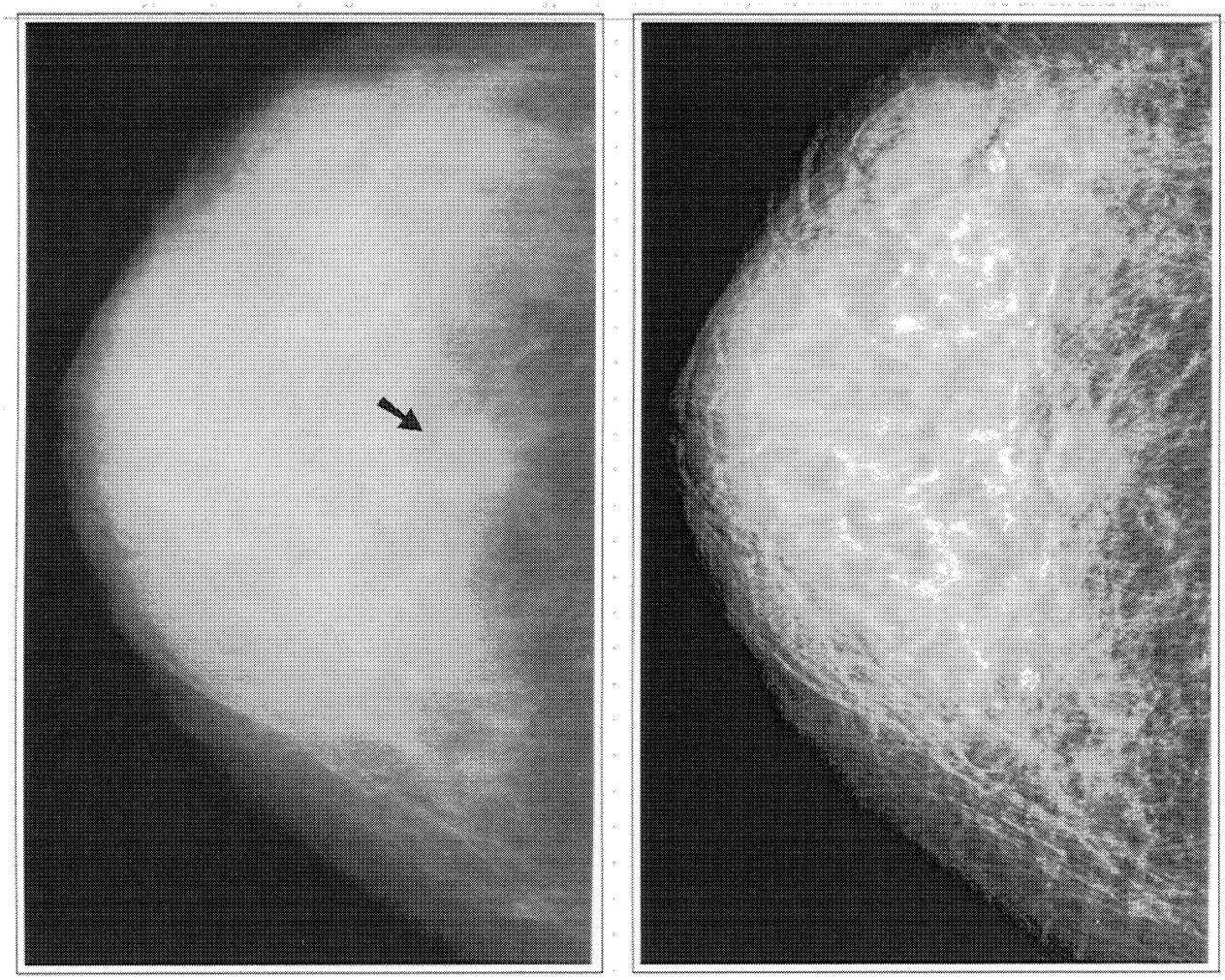

(a) Original mammogram

(b) Multiscale enhanced mammogram

Figure 10: Global image enhancement via a sub-octave wavelet transform and adaptive nonlinear processing (spicular mass, 1.5 cm).

gain values and local windows of energy, we can achieve "focused" enhancement effects. Through this nonlinear operator, SWT coefficients were modified for feature enhancement by

$$W_j^{i,m,*} f(x,y) = M_{2^j}^{i,m} \times E_{GAG}\left(\frac{W_j^{i,m} f(x,y)}{M_{2^j}^{i,m}}\right), \tag{17}$$

$$M_{2^j}^{i,m} = \max_{x,y}(|W_j^{i,m} f(x,y)|), \tag{18}$$

where $i = \{1,2\}$, $1 \leq m \leq M$, and $1 \leq j \leq J$. $W_j^{i,m,*} f(x,y)$ is a processed coefficient. Figure 7 shows a functional diagram of the generalized adaptive gain operator, at selected threshold values.

4 EXPERIMENTAL RESULTS AND ANALYSIS

First we present experimental results based on a 1-D sub-octave wavelet transform. This is used to show the de-noising capability with restored features compared to existing de-noising methods. Experimental results of SWT-based de-noising are shown in Figure 8. In the fourth plot shown in Figures 8(a)-(d), the de-noised results are overlaid with their corresponding originals. In comparison to previously published methods processing the same signals,[10] the results of the SWT-based method are noticeably improved and relatively free from artifacts.

The experimental results of enhancement with noise suppression of mammographic images via a 2-D sub-octave wavelet transform are also presented. This demonstrates the advantage of enhancement without amplifying noise, including background noise.[22] Figure 9(a) shows a region from a low contrast mammographic image containing a microcalcification cluster. Enhancement by traditional unsharp masking is presented in Figure 9(b). Figure 9(c) shows the result of SWT-based enhancement with noise suppression. Traditional unsharp masking shown in Figure 9(b) enhances the area of the microcalcification cluster but also amplifies noise. As shown in Figure 9(c), enhancement under a SWT makes barely seen microcalcification clusters more visible without amplifying noise. A global enhancement result is shown in Figure 10. Figure 10(a) is a mammogram with dense tissues and a spicular mass (1.5cm). The enhanced image is shown in Figure 10(b).

5 CONCLUSIONS

To more reliably isolate noise and identify features through scale space, we formulated and carried out sub-octave wavelet analysis. A sub-octave wavelet transform exhibited better time-frequency resolution than a traditional dyadic wavelet transform. If the number of sub-octave bands in each octave is a power of 2, we showed that a sub-octave wavelet transform of a function can be implemented by a set of FIR filters corresponding to a single pair of analysis and synthesis wavelets. FIR filters for a class of wavelets designed for a DWT were used to implement sub-octave wavelet analysis. A wavelet shrinkage scheme for noise suppression was presented and a generalization of adaptive gain processing was described to enhance features of importance to mammography without amplifying noise.

6 REFERENCES

[1] I. Daubechies, "Orthonormal bases of compactly supported wavelets", *Communications in Pure and Applied Mathematics*, vol. 41, no. 7, pp. 909–996, 1988.

[2] I. Daubechies, *Ten Lectures on Wavelets*, Number 61 in CBMS-NSF Series in Applied Mathematics. SIAM, Philadelphia, Pennsylvania, 1992.

[3] I. Daubechies, "Orthonormal bases of compactly supported wavelets II. Variations on a theme", *SIAM Journal on Mathematical Analysis*, vol. 24, no. 2, pp. 499–519, 1993.

[4] C. K. Chui, *An Introduction to Wavelets*, Academic Press, Boston, MA, 1992.

[5] S. Mallat and S. Zhong, "Characterization of signals from multiscale edges", *IEEE Transactions on Pattern Analysis and Machine Intelligence*, vol. 14, no. 7, pp. 710–732, 1992.

[6] S. Mallat and W. L. Hwang, "Singularity detection and processing with wavelets", *IEEE Transactions on Information Theory*, vol. 38, no. 2, pp. 617–643, 1992.

[7] X. Zong, A. F. Laine, E. A. Geiser, and D. C. Wilson, "De-noising and contrast enhancement via wavelet shrinkage and nonlinear adaptive gain", in *Wavelet Applications III*, Proceedings of SPIE, Orlando, FL, 1996, vol. 2762, pp. 566–574.

[8] X. Zong, E. A. Geiser, A. F. Laine, and D. C. Wilson, "Homomorphic wavelet shrinkage and feature emphasis for speckle reduction and enhancement of echocardiographic images", in *Medical Imaging: Image Processing*, Proceedings of SPIE, Newport Beach, CA, 1996, vol. 2710, pp. 658–667.

[9] D. L. Donoho and I. M. Johnstone, "Ideal spatial adaptation via wavelet shrinkage", Technical Report 400, Department of Statistics, Stanford University, 1992.

[10] R. R. Coifman and D. L. Donoho, "Translation-invariant denoising", in *Wavelets and Statistics*, Anestis Antoniadis, Ed. To appear, Springer-Verlag.

[11] A. Laine, J. Fan, and W. Yang, "Wavelets for contrast enhancement of digital mammography", *IEEE Engineering in Medicine and Biology Magazine*, vol. 14, no. 5, pp. 536–550, 1995.

[12] J. Fan and A. Laine, "Multiscale contrast enhancement and denoising in digital radiographs", in *Wavelets in Medicine and Biology*, A. Aldroubi and M. Unser, Eds., Boca Raton, Florida, 1996, pp. 163–189, CRC Press.

[13] M. Vetterli and J. Kovačević, *Wavelets and Subband Coding*, Prentice Hall, Englewood Cliffs, NJ, 1995.

[14] G. Strang and T. Nguyen, *Wavelets and Filter Banks*, Wellesley-Cambridge Press, Wellesley, MA, 1996.

[15] V. Strela, P. N. Heller, G. Strang, P. Topiwala, and C. Heil, "The application of multiwavelet filter banks to image processing", Preprint, submitted to *IEEE Trans. on Image Processing*.

[16] D. L. Donoho, "De-noising by soft-thresholding", Technical Report 409, Department of Statistics, Stanford University, 1992.

[17] D. L. Donoho and I. M. Johnstone, "Ideal denoising in an orthonormal basis chosen from a library of bases", Technical Report 461, Department of Statistics, Stanford University, 1994.

[18] S. Chen and D. L. Donoho, "Atomic decomposition by basis pursuit", Technical Report, Department of Statistics, Stanford University, 1995.

[19] R. R. Coifman and F. Majid, "Adapted waveform analysis and denoising", in *Progress in Wavelet Analysis and Applications*, Y. Meyer and S. Roques, Eds., B.P. 33, 91192 Gif-sur-Yvette Cedex, France, 1993, pp. 63–76, Editions Frontieres.

[20] J. Lu, J. B. Weaver, D. M. Healy Jr., and Y. Xu, "Noise reduction with multiscale edge representation and perceptual criteria", in *Proceedings of IEEE-SP International Symposium on Time-Frequency and Time-Scale Analysis*, Victoria, B.C., 1992, pp. 555–558.

[21] J. Lu and D. M. Healy Jr., "Contrast enhancement of medical images using multiscale edge representation", in *Wavelet Applications*, Proceedings of SPIE, Orlando, FL, 1994, vol. 2242, pp. 711–719.

[22] A. Laine, S. Song, J. Fan, W. Huda, J. Honeyman, and B. Steinbach, "Adaptive multiscale processing for contrast enhancement", in *Biomedical Image Processing and Biomedical Visualization*, Proceedings of SPIE, San Jose, CA, 1993, vol. 1905, pp. 521–532.

[23] A. F. Laine, S. Schuler, J. Fan, and W. Huda, "Mammographic feature enhancement by multiscale analysis", *IEEE Transactions on Medical Imaging*, vol. 13, no. 4, pp. 725–740, 1994.

[24] A. Laine, J. Fan, and S. Schuler, "A framework for contrast enhancement by dyadic wavelet analysis", in *Digital Mammography*, A. G. Gale, S. M. Astley, D. R. Dance, and A. Y. Cairns, Eds., Amsterdam, The Netherlands, 1994, pp. 91–100, Elsevier.